JOURNAL OF NANO- AND ELECTRONIC PHYSICS
Vol. **18** No 2, 02002(5pp) (2026)

ЖУРНАЛ НАНО- ТА ЕЛЕКТРОННОЇ ФІЗИКИ
Том **18** № 2, 02002(5cc) (2026)

OPEN ACCESS

REGULAR ARTICLE

Radiation Defects in Green GaP Light-Emitting Diodes

T.M. Zahorodnia[1], L.A. Kot[2,*], O.O. Krasnianskyi[2], P.M. Pavlovskyi[2], D.P. Stratilat[3], V.P. Tartachnyk[3]

[1] *Sumy State University, 40007 Sumy, Ukraine*
[2] *Dragomanov Ukrainian State University, 02000 Kyiv, Ukraine*
[3] *Institute for Nuclear Research, National Academy of Sciences of Ukraine, 02000 Kyiv, Ukraine*

(Received 05 January 2026; revised manuscript received 21 April 2026; published online 29 April 2026)

The results of investigations of the optical and electrical characteristics of green GaP light-emitting diodes (LEDs) grown by double liquid-phase epitaxy are presented. Low-temperature electroluminescence spectra in the wavelength range of 530 – 590 nm reveal a spectral structure with emission peaks at $\lambda_1 = 542$ nm $\lambda_2 = 554$ nm, $\lambda_3 = 576$ nm, and $\lambda_4 = 584$ nm. Injection characteristics were obtained for the listed emission wavelengths. Comparative evaluations of the radiation resistance of emissions at $\lambda_1 = 542$ nm and $\lambda_3 = 576$ nm were carried out, as well as an analysis of the differential resistance values of the diodes in the regions of the current-voltage characteristics (CVCs) exhibiting positive and negative differential resistance. The effects of electron irradiation on the reverse currents of the LEDs were analyzed, in particular the expansion of the pre-breakdown region of the CVCs and the shift of the breakdown channel toward higher voltages. The work also includes results of studies on the recovery of the electrophysical characteristics of irradiated diodes induced by isochronal annealing.

Keywords: LEDs, GaP, Radiation defects, Electroluminescence, CVCs, Spectral characteristics, Electron irradiation.

DOI: 10.21272/jnep.18(2).02002 PACS numbers: 61.80. – x, 78.60.Fi

1. INTRODUCTION

Gallium phosphide (GaP) is a semiconductor compound of the A^3B^5 (III-V) group, on the basis of which the first solid-state light sources in the visible spectral range were developed. Since the advent of industrially mass-produced (LEDs), the scope of their application has expanded significantly – from panel indicators to active elements of fiber-optic communication lines and information-processing systems.

The accelerated development of the microelectronics industry, particularly space instrumentation, as well as the design of radiation-resistant modules intended for operation in areas of increased radiation risk, requires suitable materials for the manufacture of control and measurement units, navigation devices, tracking systems and related equipment.

Compared with other III-V semiconductors, GaP possesses several important advantages, including excellent lattice matching with silicon, a wide transparency range (0.6 ÷ 11 μm), high nonlinear susceptibility, and a quasi-direct band gap ($E_g = 2.18$-2.25 eV).

Gallium phosphide is also characterized by low chemical reactivity, high hardness (1945 N/mm^2), a melting temperature of $T_m = 1467$°C, and ease of processing, which makes it a promising material for the growth of nanowires [1].

A number of methods for the fabrication of GaP nanowires have been proposed in works [2-6]. Publications [2, 3] report on the formation of such structures using Au particles; the average nanowire diameter is about 20 nm, while their length reaches tens of micrometers. GaP nanowires with diameters of 10-100 nm and lengths of several micrometers were obtained in [4] by heating Ga_2O_3 and red phosphorus. Work [5] is devoted to the investigation of the growth dynamics of heterostructured GaP and GaAs nanowires. The results of studies on the self-nucleation of InP and GaP nanowires with a low defect concentration, which are promising for optoelectronic applications, are presented in [6].

Authors of [7, 8] report on the use of GaP/Si pseudo-substrates for the growth of (N)/GaP(N) and GaAs(N)/GaP(N) quantum wells. It is also reported in [9] that the efficiency of GaP LEDs can be enhanced by using GaP with a wurtzite crystal lattice.

The results of investigations of nanostructured objects in the form of high-density quantum dots on GaP substrates are presented in [10], while studies of single quantum dots can be found in [11]. These works reveal the close proximity of two different types of optical transitions and their competition between the X and Γ valleys.

It is known that nitrogen doping plays a key role in the process of radiative recombination in GaP [12]. The authors of [13] demonstrated that a high level of isoelectronic nitrogen doping leads to the formation of

* Correspondence e-mail: l.a.kot@udu.edu.ua

Cite this article as: T.M. Zahorodnia et al., *J. Nano- Electron. Phys.* 18 No 2, 02002 (2026) https://doi.org/10.21272/jnep.18(2).02002

an impurity band which, by narrowing the band gap Eg, brings the properties of direct- and indirect-band-gap semiconductors closer together [14].

The presence of a highly sensitive depletion region within a *p-n* junction makes it possible to control the introduction of structural damage during irradiation with high-energy particles, as well as to monitor diffusion processes during annealing [15, 16].

As follows from the above brief review of previously published studies, investigations of the electrical and optical characteristics of GaP single crystals and GaP-based nanostructures remain relevant and important.

Therefore, the main objective of the present work is to study the low-temperature emission spectra and to identify the principal emission lines of the GaP(N) LEDs used in this study, as well as to evaluate their radiation resistance and to determine the features of recovery of characteristics degraded by electron irradiation.

2. EXPERIMENT

Nitrogen-doped (LEDs) were investigated. The spectral characteristics were recorded in the temperature range of 77 – 300 K using a StellarNet GreenWave series spectrometer (spectral range 350-1150 nm, 16-bit resolution, spectral resolution 0.2 nm) and an MDR-23 spectrometer.

Electron irradiation with an energy of $E = 2$ MeV was carried out using an electron accelerator. During irradiation, the sample temperature did not exceed room temperature owing to efficient air cooling.

The CVCs of the LEDs were measured using an automated setup in the temperature range of 77-300 K. Both current-source and voltage-source modes were employed, and the measurement system was controlled by a computer.

3. RESULTS

In Fig. 1 shows the spectra of GaP(N) LEDs recorded at a temperature of 77 K and excitation currents of $I = 1.5 \div 60$ mA. In the range $I = 1.5 \div 20$ mA, three broad lines can be distinguished: λ_1 =542 nm, $\lambda_2 = 554$ nm, $\lambda_3 = 576$ nm, and an inflection point, which with increasing current transitions into a fourth maximum $\lambda_4 = 584$ nm.

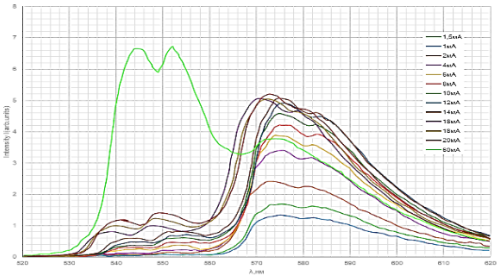

Fig. 1 – Spectral characteristics of green GaP LEDs measured at different currents ($T_{measurement}$ = 77 K)

At high currents ($I > 20$ mA), the thermal effect becomes noticeable – a decrease in the width of the crystal's band gap, accompanied by a shift of the first two lines toward longer wavelengths.

The half-width of the first line $\lambda_1 = 542$ nm, $I = 60$ mA, can be estimated based on the position of its maximum ($\Gamma = 12$ nm). It is difficult to use a similar method for the second $\lambda_2 = 554$ nm due to the distortion of its shape by the effect of self-absorption of radiation.

The first line $\lambda_1 = 542$ nm ($h\upsilon_{max} = 2.288$ eV) owes its formation to the presence of an isoelectronic nitrogen impurity, which ensures the existence of an exciton trap and, consequently, the appearance of a near-edge green signal in GaP(N) LEDs [12].

The second line $\lambda_2 = 554$ nm ($h\upsilon_{max} = 2.238$ eV) is a phonon repeat of the first $h\upsilon_{max} = 2.288$ eV with the participation of two longitudinal acoustic phonons (LA, $h\upsilon_f = 24.4$ meV)

The identical course of the dependence of the intensity of the evidence on the injection level (Fig. 2) can serve as clear confirmation of their genetic similarity

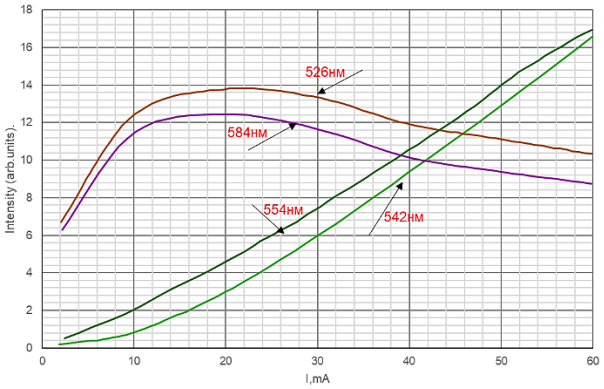

Fig. 2 – Dependence of the luminescence intensity of green GaP LEDs on the injection current

Fig. 2 builds upon and refines certain results previously published by the authors of [17].

This also applies to the last two emissions with $\lambda_3 = 576$ nm ($h\upsilon_{max} = 2.153$ eV) and $\lambda_4 = 584$ nm ($h\upsilon_{max} = 2.123$ eV)

The energy differences of their quanta $\Delta h\upsilon = 2.153$ eV - 2.123 eV = 0.03 can be correlated with the energy of the longitudinal acoustic phonon with $\varepsilon_{LA} = 24.4$ meV

Therefore, the main emission should be considered the first one with $\lambda_3 = 576$ nm; the emission with $\lambda_4 = 584$ nm is its phonon replica with the participation of longitudinal acoustic phonons. In turn, the emission with $\lambda_3 = 576$ nm is also of exciton origin, which arises as a result of the recombination of an exciton bound to a pair of closely spaced nitrogen atoms NN_1 [18].

Estimates based on temperature dependencies of the intensity of the $\lambda_{max} = 576$ nm line showed (Fig. 3) that the activation energy of the process is 17 meV and is close to the value given in [18] for a bound exciton. It is also important to note that the emission centers at $\lambda_2 = 554$ nm and $\lambda_3 = 576$ nm are mutually independent, as can be seen in (Fig. 2), where the curves $I_{int}(I$ mA) do not correlate with each other; if after $I = 20$ mA the intensity of emission with $\lambda_3 = 576$ nm begins to decrease, then for $\lambda_1 = 542$ nm it increases.

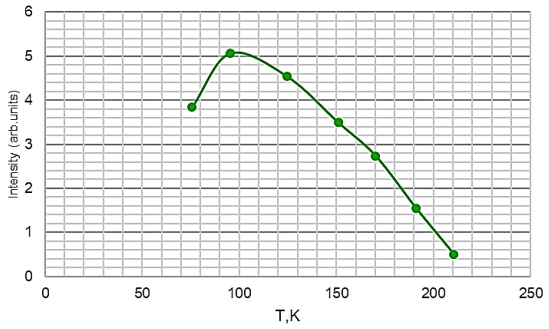

Fig. 3 – Dependence of the intensity of the λ_{max} = 576 nm line on temperature

Fig. 4 shows the relative changes in the intensity of the CD I_0/I_ϕ signal depending on the current through the diode for λ_{max} = 576 nm and λ_{max} = 542 nm

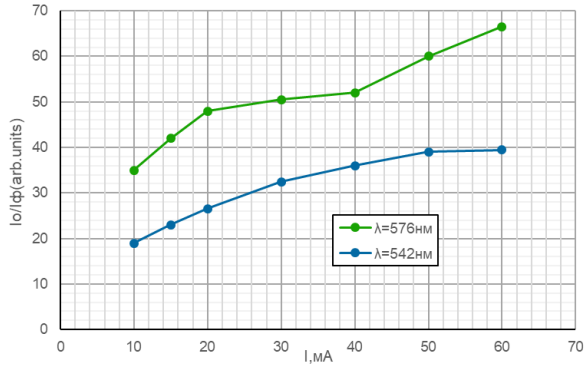

Fig. 4 – Dependence of the relative intensity of luminescence I_0/I_ϕ of lines and λ_{max} = 576 nm and λ_{max} = 542 nm on current

It can be seen, that the radiation resistance of both bands I_0/I_ϕ increases with the increase in injection current due to the strengthening of the shielding effect of radiation defects by free carriers and the corresponding weakening of the destructive effect of radiation damage on the intensity of radiative recombination.

The exciton recombination band on closely spaced NN_1 λ_{max} = 542 nm atoms are more resistant to radiation than the recombination band of excitons localized on isolated N atoms (Fig. 4). The result seems obvious when considering that the depth of the exciton at the center of NN_1 is almost six times greater than at an isolated N atom [18].

Fig. 5 shows the family of CVCs GaP(N) LEDs obtained within the range (95 – 300 K); the measurement mode was a generator of current. After cooling the sample below T = 135 K, an S-type negative differential resistance section is formed on the CVCs, and with the temperature drop to 95 K, areas of positive and negative slope with differential resistances can be distinguished on the CVCs, for which the average values of the ratios $R_{diff.irradiated}/R_{diff.irradiated}$ are

$$\frac{R^{+}_{diff.irradiated\text{p}}}{R^{+}_{diff.irradiated}} = 11{,}67 \qquad \frac{R^{-}_{diff.irradiated}}{R^{-}_{diff.irradiated}} = 9{,}43$$

It is seen that irradiation of the diode leads to an increase in both the positive and the negative value of the differential resistance (dU/dI). It is also known [16] that deep levels of radiation defects in n- and p-type GaP single crystals compensate its electrical conductivity, therefore the increase of R^+ is an obvious reaction of the device base to irradiation.

The increase in R^- can only be discussed in terms of certain assumptions, as there is currently no consensus on the mechanism responsible for the formation of negative differential resistance (NDR) in GaP LEDs.

If one adheres to the model of double injection of carriers into the depleted region of the p-n junction, then, with a large difference between the capture cross-sections of electrons and holes at the main recombination level, the flux of carriers of one type becomes saturated as the injection level increases. In this case, the lifetime of carriers of the opposite type increases rapidly, which leads to their filling of the high-resistance depleted region; the voltage across the sample decreases against the background of a rising current.

The released heat plays the role of a positive feedback factor, and an S-shaped region of current-controlled negative differential resistance develops on the CVCs.

The introduction of deep levels by electron irradiation compensates the electrical conductivity not only of the base regions of the diode; the compensation equally concerns the current filament that forms the S-shaped region of the CVCs, and the increase in its resistance appears on the graph in Fig. 5 as an increase of R^-.

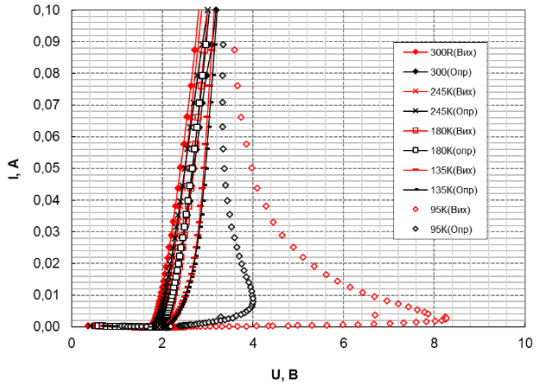

Fig. 5 – CVCs of a green GaP LED irradiated with electrons $\Phi = 2{,}05 \times 10^{15}$ cm^{-2}, measured at different temperatures

According to the Shockley formula for an ideal junction

$$I = I_s(e^{\frac{qu}{nkt}} - 1)$$

where $\boldsymbol{I_S}$ – reverse saturation current (thermal current, minority carrier current), and $\boldsymbol{n}$ is the diode ideality factor that determines the mechanism of current transport through the junction. To obtain it, the dependence of the photocurrent generated by the LED light flux on the applied voltage was measured in the interval of photocurrent values of about $10^{-5} \div 10^{-10}$ A. After U = 2,5 V $I_\Phi(U)$ for the initial and irradiated LEDs ($\Phi = 3 \times 10^{14}$ cm^{-2}) reaches saturation, and the ideality factor in the region of small currents is n = 1.67. At such a value of n, the current that causes emission is

controlled by diffusion and recombination in the space-charge region.

An almost twofold increase in irradiation dose ($\Phi = 5{,}9 \times 10^{14}$ cm^{-2}) leads to a sharp increase of n ($n = 4.18$). Now the main mechanism of current formation becomes tunneling of carriers through the damaged regions of the space-charge region.

The reverse branch of the CVCs of the investigated LEDs within the ranges $\Delta I = 2 \times 10^{-10} \div 3 \times 10^{-10}$ A and $\Delta U = 0 \div 25$ V, a characteristic saturation current region I_S and a breakdown region are observed, which arise as a result of reaching the breakdown voltage $U = U_{br}$. In the initial diode, the saturation current is $I_S \sim 3 \times 10^{-10}$ A (Fig. 6 (a)); electron irradiation with a fluence of $\Phi = 2 \times 10^{16}$ cm^{-2} reduces this value only by approximately a factor of one and a half (Fig. 6 (b)). The introduction of radiation defects is accompanied by a broadening of the transition region in Fig. 6 (b) from an almost constant value of I_S to I_{br}, which may be a consequence of interlevel carrier tunneling stimulated by the presence of radiation damage.

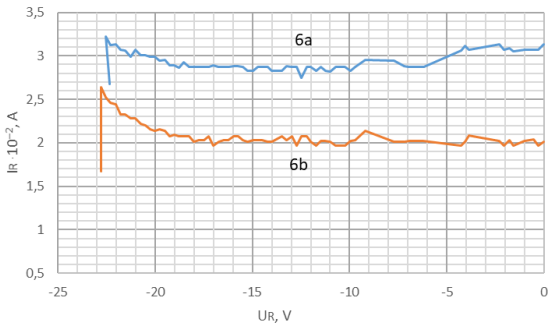

Fig. 6 – Reverse CVCs of the initial green GaP LED (a) and the LED irradiated with electrons $\Phi = 2 \times 10^{16}$ cm^{-2}(b) ($T_{meas} = 77$ K)

Measurements show that, in the vast majority of samples, an increase in temperature from 77 to 300 K leads to a shift of the breakdown regions toward higher voltages, which is an argument in favor of the avalanche nature of the breakdown. Fig. 7 shows the dependence of the breakdown current on the temperature of isochronal annealing of the LEDs, taken in the range from $U_1 = 24$ V to $U_2 = U_{br} = 24{,}2$ V. The decrease in breakdown current is a consequence of filling of the breakdown channel with the decay products of radiation-induced defect clusters and the corresponding increase in the scattering intensity of carriers.

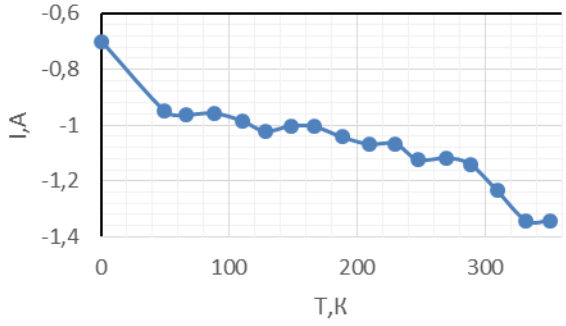

Fig. 7 – Dependence of the breakdown current of a green GaP LED on the annealing temperature.

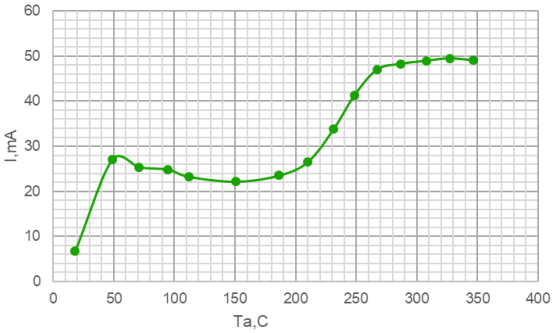

Fig. 8 – Annealing of a green GaP LED

Fig. 8 shows the results of the restoration of the CVCs of the LED irradiated with electrons. Annealing was carried out in the interval 20 ÷ 350°C at a constant current $I = 6 \times 10^{-2}$ A; while the annealing process was monitored by measuring the voltage.

The final measurement results are shown in Fig. 8 as the dependence of the diode current on the annealing temperature $U(T)$.

Its pronounced three-stage behavior indicates the presence of three diffusion components in the overall recovery process. The first, sharp stage in the temperature range of 20-50°C, during which the current increases, is most likely associated with the annihilation of defects with low activation energy, primarily surface defects involved in the formation of leakage currents. Some of these defects disappear at sinks, while others form stable complexes, thereby increasing the electrical strength of the diode in the subsequent stage at 50-150 C.

The main recovery stage corresponds to the current increase observed in the temperature range of 150-300 C. This behavior is attributed to the decompensation of the n- and p-regions of the diode caused by the migration of V_P and V_{Ga} defects toward sinks, followed by a gradual restoration of the potential barrier height.

4. CONCLUSIONS

Monocrystalline GaP is currently the subject of intensive research aimed at improving methods for the formation of GaP-based nanostructures, including quantum wells, nanowires, and quantum dots.

Owing to the simplicity of their structure and growth technology, GaP LEDs serve as convenient model objects for studying charge transport mechanisms and recombination processes in more complex binary compounds containing quantum wells. In addition, they are useful for relative assessments of the radiation resistance of other solid-state light sources.

In the present work, emission lines at $\lambda_1 = 542$ nm and $\lambda_2 = 554$ nm were identified. The former originates from the recombination of an exciton bound to a nitrogen impurity, while the latter represents the phonon replica of this transition involving an acoustic phonon. Emission at $\lambda_3 = 576$ nm corresponds to excitonic recombination on NN_1 pairs. It was shown that the NN_1 emission line exhibits higher radiation resistance compared with the emission line of excitons bound to isolated nitrogen atoms. The appearance of a NDR region in the CVCs,

which is typical for GaP LEDs in the low-temperature range ($T \leq 90$ K), can be attributed to the double injection of charge carriers into the depletion region of the *p-n* junction. In this region, the probability of carrier capture of one type significantly exceeds that for carriers of the opposite type. The resulting increase in current and the associated heat generation act as a positive feedback mechanism.

Electron irradiation of the LEDs leads to a decrease in the reverse current magnitude; however, at an irradiation dose of $\Phi = 5 \times 10^{-14}$ cm^{-2}, an increase in the tunneling component of the reverse current is observed.

The temperature-induced shift of the breakdown region of the reverse CVCs, $I(U_{rev})$, toward higher voltages indicates an avalanche breakdown mechanism.

Restoration of the CVCs of GaP LEDs using isochronal annealing demonstrates a three-stage behavior. At the first stage (20-50 °C), defects predominantly localized at the surface of the *p-n* junction is removed. The third stage (150-300°C) is associated with the decompensation of the *n*- and *p*-regions under conditions of increased defect mobility.

The intermediate annealing interval (50-150 °C) may result from interactions between simple structural defects that become mobile during the first stage, leading to the formation of defect complexes which subsequently dissociate during the third, main annealing stage.

REFERENCES

1. K.A. Dick, *Progr. Cryst. Growth Charact. Mater.* **54**, 138 (2008) https://doi.org/10.1016/j.pcrysgrow.2008.09.001.
2. F.M. Davidson, R. Wiacek, B.A. Korgel, *Chem. Mater.* **17**, 230 (2005) https://doi.org/10.1021/cm0486262.
3. J. Johansson, L.S. Karlsson, C. Patrik T. Svensson, T. Mårtensson, B.A. Wacaser, K. Deppert, L. Samuelson, W. Seifert, *Nat. Mater.* **5**, 574 (2006) https://doi.org/10.1038/nmat1677.
4. B. Liu, L. Wei, Q. Ding, J. Yao, *Nanotechnology* **15**, 1745 (2004) https://doi.org/10.1088/0957-4484/15/12/007.
5. M.A. Verheijen, G. Immink, T. De Smet, M.T. Borgström, E.P.A.M. Bakkers, *J. Am. Chem. Soc.* **128**, 1353 (2006) https://doi.org/10.1021/ja057157h.
6. Z. Liu, K. Sun, W. Jian, D. Xu, Y. Lin, J. Fang, *Chem. A Eur. J.* **15**, 4546 (2009) https://doi.org/10.1002/chem.200900190.
7. T. Nguyen Thanh, C. Robert, W. Guo, A. Létoublon, C. Cornet, G. Elias, A. Ponchet, T. Rohel, N. Bertru, A. Balocchi, O. Durand, J.S. Micha, M. Perrin, S. Loualiche, X. Marie, A. Le Corre, *J. Appl. Phys.* **112**, 053521 (2012) https://doi.org/10.1063/1.4751024.
8. K. Umeno, Y. Furukawa, A. Wakahara, R. Noma, H. Okada, H. Yonezu, Y. Takagi, H. Kan, *J. Cryst. Growth* **311**, 1748 (2009) https://doi.org/10.1016/j.jcrysgro.2008.10.075.
9. S. Assali, D. Kriegner, I. Zardo, S. Plissard, M.A. Verheijen, J. Stangl, J.E.M. Haverkort, E.P.A.M. Bakkers, *Proc. SPIE* **9174**, Nanoepitaxy: Materials and Devices VI, 917405 (2014) https://doi.org/10.1117/12.2063865.
10. T. Nguyen Thanh, C. Robert, C. Cornet, M. Perrin, J.M. Jancu, N. Bertru, J. Even, N. Chevalier, H. Folliot, O. Durand, A. Le Corre, *Appl. Phys. Lett.* **99**, 143123 (2011) https://doi.org/10.1063/1.3646911.
11. C. Robert, C. Cornet, P. Turban, T. Nguyen Thanh, M.O. Nestoklon, J. Even, J.M. Jancu, M. Perrin, H. Folliot, T. Rohel, S. Tricot, A. Balocchi, D. Lagarde, X. Marie, N. Bertru, O. Durand, A. Le Corre, *Phys. Rev. B* **86**, 205316 (2012) https://doi.org/10.1103/PhysRevB.86.205316.
12. A.A. Bergh, P.J. Dean, *Light-Emitting Diodes* (Clarendon Press: Oxford: 1976).
13. Y. Zhang, B. Fluegel, A. Mascarenhas, H. Xin, C. Tu, *Phys. Rev. B* **62**, 4493 (2000) https://doi.org/10.1103/PhysRevB.62.4493.
14. S. Boyer-Richard, *Carrier injection in GaAsPN/GaPN Quantum Wells on Silicon* (2011). https://www.academia.edu/18188767/Carrier_injection_in_GaAsPN_GaPN_quantum_wells_on_Silicon.
15. V.V. Volkov, V.Ya. Opylat, V.P. Tartachnyk, I.I. Tychyna, *High Purity Substances* No 2, 60 (1989).
16. O.V. Konoreva, O.I. Radkevych, V.I. Slisenko, V.P. Tartachnyk, *Naukova Dumka* 200 (2021).
17. P.H. Lytovchenko, I.V. Petrenko, D.P. Stratilat, V.P. Tartachnyk, M.Ye. Chumak, *Nucl. Phys. At. Energy* **25** No 2, 134 (2024) https://doi.org/10.15407/jnpae2024.02.134.

Радіаційні дефекти у зелених світлодіодах GaP

Т.М. Загородня[1], Л.А. Кот[2], О.О. Краснянський[2], П.М. Павловський[2], Д.П. Стратилат[3], В.П. Тартачник[3]

[1] *Сумський державний університет, 40000, Суми, Україна*
[2] *Український державний університет імені Михайла Драгоманова, 02000, Київ, Україна*
[3] *Інститут ядерних досліджень, 02000, Київ, Україна*

У роботі наведені результати досліджень оптичних та електрофізичних характеристик зелених СД GaP, вирощених подвійною рідинною епітаксією. На низькотемпературних спектрах електролюмісценції в межах 530-590 нм виявлена структура з $\lambda_1 = 542$ нм, $\lambda_2 = 554$ нм, $\lambda_3 = 576$ нм та $\lambda_4 = 584$ нм, одержані інжекційні характеристики для перерахо-ваних довжин хвиль. Зроблені порівняльні оцінки радіаційної стійкості випромінювань з $\lambda_1 = 542$ нм і $\lambda_3 = 576$ нм, а також величин диференційних опорів діодів на ділянках ВАХ з додатнім та від'ємним опором. Розглянуто результати впливу електронного опромінення на зворотні струми СД, а саме: розши-рення передпробійної ділянки ВАХ та зсув пробійного каналу у бік вищих напруг. Робота також містить матеріали досліджень відновлення електрофізичних характеристик опромі-нених діодів, спричинених ізохронним відпалом.

Ключові слова: Світлодіод, GaP, Електролюмісценція, Вольт-амперні характеристики, Спектральні характеристики, Опромінення.